Documentation of the Solutions to the SFPE Heat Transfer Verification Cases

Prepared by a Task Group of the SFPE Standards Making Committee on Predicting the Thermal Performance of Fire Resistive Assemblies

Ann Jeffers
University of Michigan

Ulf Wickström
Luleå University/SP Research Institute

Kevin McGrattan
National Institute for Standards and Technology

Table of Contents

Executive Summary

In 2012, a Task Group was formed by the SFPE Standards Making Committee for Predicting the Thermal Performance of Fire Resistive Assemblies to develop a set of verification cases to be published in the *SFPE Standard on the Development and Use of Methodologies for Predicting the Thermal Performance of Fire Resistive Assemblies*. The Task Group compiled existing verification problems, made modifications to problem statements for consistency and completeness, developed new verification problems to address physics that were not captured in existing verification problems, and derived solutions to all cases, ensuring that the published solution was within an acceptable degree of accuracy.

This report documents the work that was performed by the Task Group to determine the solutions to the verification cases that appear in the Annex of the Standard. All verification problems were evaluated by two calculation methods. For problems in which an analytical solution exists, the analytical solution was compared to a numerical solution to verify the accuracy of the solution. For problems in which no analytical solution exists, the cases were modeled by two different numerical methods and the results were compared to demonstrate that the two methods yield the same result within an acceptable tolerance. Modeling assumptions, convergence studies, and comparisons between calculation methods are documented in the report. Input files for numerical models have been archived and are available for download on the SFPE website at http://www.sfpe.org/.

1. Introduction

The SFPE Standards Making Committee for Predicting the Thermal Performance of Fire Resistive Assemblies undertook the task of drafting a standard to regulate the development and use of methods for predicting the thermal performance of structural and fire resistive assemblies. The standard addresses the general requirements of the method of heat transfer analysis, the input data and boundary conditions in the model, the verification and validation procedure, and the application and documentation of the method.

A chapter of the standard is dedicated to verification, which requires the user to verify the method of heat transfer analysis against a series of verification cases that appear in the annex of the standard. *Verification* is defined as "the process of determining the degree of accuracy of the solution of the governing equations." The verification procedure involves modeling a series of problems with known solutions and demonstrating that the calculation method converges to the exact solution for each problem as the temporal and spatial resolution of the model is increased.

The challenge to developing a set of standard verification cases is that most fire safety engineering applications involve complexities (e.g., nonlinear boundary conditions and material effects) that prohibit the formulation of a close-formed analytical solution. As a result, the solution to a problem can only be obtained numerically, and the accuracy of the solution can only be verified by comparison to another numerical solution. If two numerical methods are in agreement, it is never fully known whether the agreed-upon solution is the exact solution to the problem, although confidence in the accuracy of the solution improves as the solution is verified by additional calculation methods.

In moving forward with the development of a standard verification scheme for fire safety engineering applications, a Task Group of the SFPE Standards committee was formed to compile existing verification problems, make modifications to problem statements for consistency and completeness, develop new verification problems to address physics that were not captured in existing verification problems, and derive solutions to all cases, ensuring that the published solution is reported within an acceptable degree of accuracy. This report documents the work that was performed to derive the published solutions that appear in the standard.

1.1 Review of Existing Verification Cases

Various classical texts on heat transfer analysis (e.g., Carslaw and Jaegar, 1969) have presented analytical and numerical solutions to a number of heat transfer problems. However, such texts may have limited applicability in fire safety engineering due to the simplicity of the problems that are presented. In particular, the boundary conditions and material effects may not capture a wide range of effects that are necessary in fire safety engineering, such as mixed convection and radiation from a surrounding gas whose temperature varies in time (e.g., the standard fire test) or latent heat due to moisture evaporation (e.g., as appears in heated concrete).

Due to the limitations of classical heat transfer problems, a number of verification problems have been proposed by various individuals from the fire safety engineering community. Wickström and Pålsson (1999) presented a suite of heat transfer problems that were used to verify the TASEF software. The problems have since been used in the verification of other software packages, including SAFIR (Pintea and Franssen, 1997) and HEATING (Trelles et al., 2003). The cases published by Wickström and Pålsson involve 1D and 2D heating in homogenous and composite sections with various material effects, including temperature-dependent conductivity and latent heat due to moisture evaporation. Some of the cases also involve radiation and convection across voids. A few verification cases appear in the Annex to the German Eurocode Standard *DIN EN 1991-1-1-2* (2010). The cases involve 1D and 2D heating in homogeneous and composite sections and involve constant and temperature-dependent material effects. Additional verification cases can be found in the literature. For example, Jeffers and Sotelino (2009) and Jeffers (2013) presented various 1D, 2D, and 3D problems that were used to verify a finite element formulation for the case of non-uniform heating.

From the review of heat transfer verification cases, it can be concluded that existing cases come from a variety of sources (i.e., reports, standards, and journal papers) that are not always readily accessible to a practicing engineer. Some of the published cases are incomplete, as pertinent details are missing or the cases do not capture all of the necessary physics. Furthermore, because the cases were developed by various authors, there are some inconsistencies in modeling assumptions and the published solutions are reported with varying degrees of accuracy.

Therefore, after compiling the existing verification cases, the Task Group selected the most appropriate verification cases to be included in the standard and developed new verification cases to address physics that were not captured in the existing verification cases. Problem statements were modified from original sources in many instances for completeness and consistency in the modeling assumptions. A comprehensive analysis was performed to derive the solutions to all of the problems and to ensure that the published solution was reported to an acceptable degree of accuracy. A summary of the selected verification cases is given in Section 1.2, and an overview of the procedure that was used to derive solutions to the verification cases is given in Section 1.3.

1.2 Summary of Verification Cases in the Standard

A total of sixteen verification cases were proposed for inclusion in the Annex of the SFPE *Standard on the Development and Use of Methodologies to Predict the Thermal Performance of Structural and Fire Resistive Assemblies*. As shown in Table 1, the verification cases involve a range of boundary conditions, material effects, and geometric effects to capture the most common behaviors that are encountered when modeling the thermal response of structural and fire resistive assemblies. In particular, the verification cases include lumped mass, 1D, 2D, and 3D heat transfer in homogenous and non-homogenous solids. Rectangular and axisymmetric coordinates are used in the 1D and 2D cases. The problems include temperature-dependent material effects, latent heat due to moisture evaporation, and heat transfer in voids.

Table 1. Verification Cases

Case	Description
1	Lumped mass subjected to standard fire
2	Lumped mass subjected to incident flux
3	1D heat transfer with cooling by convective
4	1D axisymmetric heat transfer by convection
5	2D axisymmetric heat transfer by convection and radiation
6	2D heat transfer with cooling by convection
7	2D heat transfer by convection and radiation
8	2D heat transfer with temperature-dependent conductivity
9	2D heat transfer in a composite section with temperature-dependent conductivity
10	2D axisymmetric heat transfer with non-uniform heat flux
11	Lumped mass with moisture evaporation
12	1D heat transfer with moisture evaporation
13	2D heat transfer with moisture evaporation
14	2D heat transfer in a composite section with moisture evaporation and temperature-dependent conductivity
15	2D heat transfer in a composite section with cavity radiation
16	3D heat transfer with non-uniform heat flux

1.3 Solution Methodology

Most of the verification cases do not have close-formed analytical solutions due to various complexities, including nonlinear boundary conditions and temperature-dependent material effects. Therefore, the solutions to almost all of the cases had to be obtained numerically. In summary, the following rules were applied to determine the published solutions:

- If an analytical solution exists, the published solution was calculated directly from the analytical solution and verified by finite element analysis.
- If an analytical solution does not exist, the case was modeled by at least two different numerical methods. The results from the numerical analyses were compared. If the methods yielded results that were within a specified tolerance, the numerical solution was deemed acceptable for publication in the Standard.

Numerical methods that were used to solve the verification problems included finite difference (for the lumped mass problems) and finite element methods. For the finite difference calculations, the governing equations are given in this report. The finite element analyses were conducted in Abaqus, v. 6.11 (2011) and TASEF (Sterner and Wickström, 1990). Abaqus and TASEF have a number of fundamental differences in their algorithms and formulations. Most importantly, Abaqus uses an implicit solver for transient thermal problems whereas TASEF uses an explicit solver. The implicit solver in Abaqus is unconditionally stable but requires iterations for convergence for nonlinear problems. The explicit solver in TASEF requires a relatively small

time increment for stability but is able to solve the governing equations directly without iteration. Abaqus and TASEF also differ in the inclusion of latent heat effects as well as the manner in which cavity radiation is specified. The differences in the solving techniques between the two programs and the similarities of the calculated temperatures help to build confidence in the solutions that were obtained numerically.

2. Governing Equations

The governing equations for the verification problems are given as follows. Additional details can be found in Carslaw and Jaeger (1969), Lattimer (2008), and Wickström (2008).

Heat conduction within an isotropic solid is governed by the following equation (the nomenclature is provided in (Table 2):

$$\rho c \frac{\partial T}{\partial t} = \frac{\partial}{\partial x}\left(k \frac{\partial T}{\partial x}\right) + \frac{\partial}{\partial y}\left(k \frac{\partial T}{\partial y}\right) + \frac{\partial}{\partial z}\left(k \frac{\partial T}{\partial z}\right) \tag{1}$$

In cylindrical coordinates where the temperature varies in the radial coordinate only, Eq. (1) can be written:

$$\rho c \frac{\partial T}{\partial t} = \frac{\partial}{\partial r}\left(r\, k \frac{\partial T}{\partial r}\right) \tag{2}$$

The boundary condition in both Cartesian and cylindrical coordinate systems is typically expressed:

$$-k \frac{\partial T}{\partial n} = \dot{q}'' \tag{3}$$

where n denotes the normal direction pointing into the solid and $\dot{q}''$ is the net heat flux onto the solid surface.

For the problems to follow, the heat flux, $\dot{q}''$, is expressed in one of two ways. For cases where the solid object is completely surrounded by an optically thick gas whose temperature varies only as a function of time, $T_{\mathrm{f}}(t)$, the heat flux is given by:

$$\dot{q}'' = \varepsilon\sigma\left(\bar{T}_{\mathrm{f}}^4 - \bar{T}_{\mathrm{s}}^4\right) + h(T_{\mathrm{f}} - T_{\mathrm{s}}) \tag{4}$$

where T_{f} and $\bar{T}_{\mathrm{f}}$ are the gas temperature in °C and K, respectively, and T_{s} and $\bar{T}_{\mathrm{s}}$ are the calculated surface temperature in °C and K, respectively. For example, the standard ISO 834 fire is given by the following time-temperature curve:

$$T_{\mathrm{f}}(t) = 20 + 345 \log\left(\frac{8t}{60} + 1\right) \tag{5}$$

where T_f is in °C, and t is the time in seconds. For the radiant heater case where the incident radiation is specified, the boundary condition should be expressed in the form of the incident radiative heat flux $\dot{q}''_{\mathrm{inc}}$ by

$$\dot{q}'' = \varepsilon(\dot{q}''_{inc} - \sigma\bar{T}_{\mathrm{s}}^4) + h\left(T_{\mathrm{g}} - T_{\mathrm{s}}\right) \tag{6}$$

Note that $\bar{T}_s$ is absolute temperature of the surface in Kelvin, K. The convective heat transfer coefficient, *h*, is used to describe convective heat transfer to the sample surface as proportional to the temperature difference between the gas temperature and the surface temperature.

Alternatively Eq. 6 may be written as

$$\dot{q}'' = \varepsilon\sigma(\bar{T}_{\mathrm{r}}^4 - \bar{T}_{\mathrm{s}}^4) + h\left(T_{\mathrm{g}} - T_{\mathrm{s}}\right) \tag{7}$$

where the black body radiation temperature is defined as $\bar{T}_r = \sqrt[4]{\frac{\dot{q}''_{inc}}{\sigma}}$.

Table 2. Nomenclature.

Symbol	Quantity	Units
A/V	surface area to volume ratio	1/m
c	specific heat	J/(kg·K)
h	heat transfer coefficient	W/(m^2·K)
k	thermal conductivity	W/(m·K)
$\dot{q}''$	heat flux	W/m^2 or kW/m^2
r	radial coordinate	m
T	temperature	°C
$\bar{T}$	temperature	K
t	time	s
(x, y, z)	Cartesian coordinates	m
σ	Stefan-Boltzmann constant	5.67×10^{-8} W/(m^2·K^4)
ρ	density	kg/m^3
ε	emissivity	dimensionless

3. Published Solutions to the Verification Cases

3.1 Case 1 – Lumped Mass Subjected to Standard Fire

3.1.1. Problem Statement

A plate ($\rho = 7850\ \mathrm{kg/m^3}, c = 520\ \mathrm{J/(kg{\cdot}K)}, \varepsilon = 0.7$) that has a thickness of 4 cm and an initial temperature of 20 °C is heated on the top and bottom surfaces according to the standard ISO 834 fire curve, Eq. (5). As the thermal conductivity of the material is relatively large, the temperature in the section, T, can be taken as uniform. For the convection heat transfer coefficient $h = 25\ \mathrm{W/(m^2 \cdot K)}$, calculate the temperature of the plate as a function of time and compare to the values given in Table 3.

Table 3. Reference Values

Time (s)	Temperature (°C)
0	20.
300	97.8
600	234.4
900	390.2
1200	539.7
1500	662.9
1800	751.9

3.1.2. Modeling Approach

A finite difference model was developed and verified by a finite element analyses conducted in Abaqus and TASEF.

For the finite difference model, the radiation term was linearized in terms of an effective heat transfer coefficient h_r, which is given according to:

$$h_r = \varepsilon\sigma(T + T_f)(T^2 + T_f^2) \tag{8}$$

Combining Eqs. (1), (5), and (8) and using a finite difference approximation for the temperature gradient dT/dt gives the temperature at step i as:

$$T_i = T_{i-1} + \left(\frac{2}{d\rho c}\right)(h + h_{r,i-1})(T_f - T_{i-1})\Delta t \tag{9}$$

where d is thickness of the specimen. The temperature in Table 3 was calculated by Eq. (9), with the time step Δt reduced until the solution converged to within 0.1 °C. The finite difference model converged at a time step of 0.25 s. The 2-norm error is plotted as a function of time step, and it can be seen that the lumped mass finite difference model exhibits first-order accuracy (i.e., $O(\Delta t)$) in time.

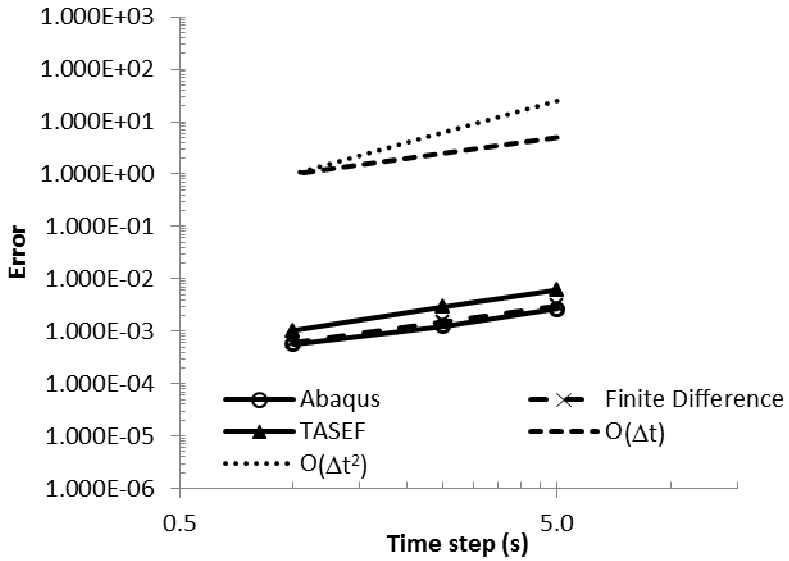

Figure 1. Order of Accuracy of the Finite Difference, Abaqus, and TASEF Models

Because Abaqus does not have a lumped mass model, a 2D finite element model was generated with linear heat transfer elements and uniform temperature was imposed throughout the model using a tie constraint. A lumped mass model was also generated in TASEF. Convergence studies were performed, and it was determined that a time step of 0.5 s resulted in a solution that converged with 0.1 °C accuracy in the Abaqus model and 1 °C in the TASEF model. The 2-norm errors for the Abaqus and TASEF models are plotted in Figure 1, and it can be seen that Abaqus and TASEF exhibit first-order accuracy in time. The calculated error is slightly larger for the TASEF model because the temperature output from TASEF is only reported with 1 °C precision.

3.1.3 Comparison of Results

In Table 4, the temperatures calculated by the finite difference model (i.e., Eq. (9)) are compared to the temperatures calculated by Abaqus and TASEF. The temperature difference between the Abaqus model and the finite difference model is within 0.1 °C, as shown in Table 4. The TASEF solution is within 1 °C of the finite difference and Abaqus solutions.

Table 4. Comparison between the Finite Difference, Abaqus, and TASEF Models

Time (s)	Calculated Temperature (°C)			Difference between the Abaqus and Finite Difference Models (°C)
	Finite Difference	Abaqus	TASEF	
0	20.0	20.0	20	0.0
300	97.8	97.7	98	-0.1
600	234.4	234.4	235	0.0
900	390.2	390.1	390	-0.1
1200	539.7	539.6	540	-0.1
1500	662.9	662.8	663	-0.1
1800	751.9	751.8	752	-0.1

3.2 Case 2 – Lumped Mass Subjected to Incident Flux

3.2.1 Problem Statement

A 1 cm thick horizontal flat plate ($\rho = 7850$ kg/m^3, $c = 560$ J/(kg·K), $\varepsilon = 0.9$) with an initial temperature of 20 °C is exposed from above with a radiant heater set to an incident flux of $\dot{q}''_{\text{inc}}$ = 50 kW/m^2. The net heat flux to the top surface of the plate is given by Eq. (6). The gas temperature is 20 °C and $h = 12$ W/(m^2 · K). Assuming that the bottom and sides of the plate are perfectly insulated, and that the thermal conductivity of the material is sufficiently large to assume a uniform temperature with depth, calculate the temperature of the plate as a function of time and compare to the values given in Table 5.

Table 5. Reference Values

Time (s)	Temperature (°C)
0	20.0
180	195.0
360	347.3
540	466.2
720	547.5
900	596.6

3.2.2. Modeling Approach

A finite difference model was developed from Eqs. (1) and (6) and verified by finite element analyses conducted in Abaqus and TASEF.

For the finite difference model, the governing equation based on Eqs. (1) and (6) is:

$$\rho c \frac{\mathrm{d}T}{\mathrm{d}t} = \left(h\left(T_{\mathrm{g}} - T\right) + \varepsilon\left(\dot{q}''_{\text{inc}} - \sigma T^4\right)\right) A/V \tag{10}$$

Using a finite difference approximation for the gradient dT/dt gives the temperature at step i as:

$$T_i = T_{i-1} + \frac{1}{d\rho c}\left[\left(T_g - T_{i-1}\right) + \varepsilon\left(\dot{q}''_{\text{inc}} - T_{i-1}^4\right)\right]\Delta t \tag{11}$$

where d is thickness of the specimen. The temperature in Table 5 was calculated by Eq. (11), with the time step Δt reduced until the solution converged to within 1 °C. The solution converged at a time step of 5 s. As illustrated in Figure 2, the lumped mass model exhibits first-order accuracy (i.e., $O(h)$) in time.

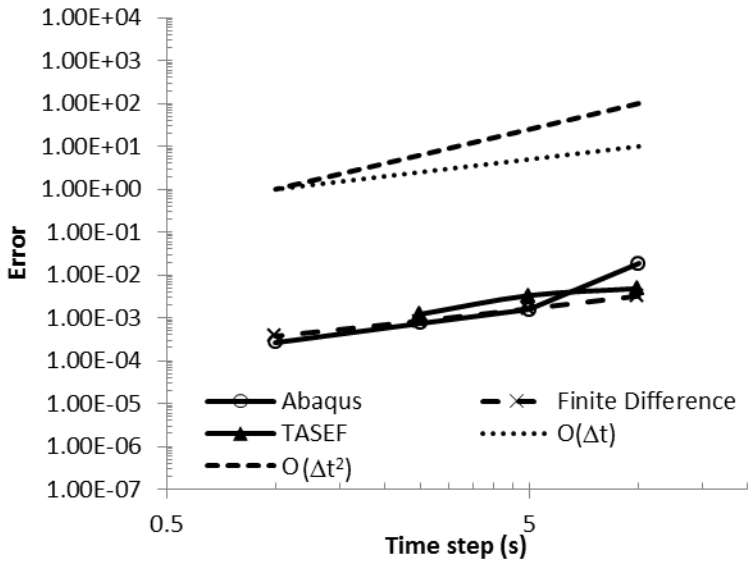

Figure 2. Order of Accuracy for the Finite Difference, Abaqus, and TASEF Models

Because Abaqus does not have a lumped mass model, a 2D finite element model was generated with linear heat transfer elements and uniform temperature was imposed throughout the model using a tie constraint. A lumped mass model was also generated in TASEF. Convergence studies were performed, and it was determined that a time step of 1 s resulted in a solution that converged within 0.5 °C accuracy for the Abaqus model and 1 °C for the TASEF model. The 2-norm errors for the Abaqus and TASEF models are plotted in Figure 2, and it can be seen that Abaqus and TASEF exhibit first-order accuracy in time. The calculated error is slightly larger for the TASEF model because the temperature output from TASEF is only reported with 1 °C precision.

3.2.3 Comparison of Results

In Table 6, the temperatures calculated by the finite difference model (i.e., Eq. (11)) are compared to temperatures calculated by Abaqus and TASEF. It can be seen that the temperature difference between the Abaqus model and the lumped mass model is within 0.1 °C. The TASEF solution is within 1 °C of the finite difference and Abaqus solutions.

Table 6. Comparison between the Finite Difference, Abaqus, and TASEF Models

Time (s)	Calculated Temperature (°C)			Difference between the Abaqus and Finite Difference Models (°C)
	Finite Difference	Abaqus	TASEF	
0	20.0	20.0	20	0.0
180	195.0	194.9	195	-0.1
360	347.3	347.3	348	0.0
540	466.2	466.2	467	0.0
720	547.5	547.4	548	-0.1
900	596.6	596.5	597	-0.1

3.3 Case 3 – 1D Heat Transfer with Cooling by Convection

3.3.1 Problem Statement

A 1 m thick slab of material ($k = 1$ W/(m·K), $\rho = 1000$ kg/m^3, $c = 1$ J/(kg·K), $\varepsilon = 0$) with an initial temperature of 1000 °C is cooled via convection only. The surrounding air temperature is 0 °C and $h = 1$ W/(m^2·K). Assuming that the back and sides of the slab are perfectly insulated, calculate the temperature of the back side of the slab as a function of time and compare to the values given in Table 7.

Table 7. Reference Values

Time (s)	Temperature (°C)
0	1000.0
60	999.3
300	891.8
600	717.7
900	574.9
1200	460.4
1500	368.7
1800	295.3

3.3.2. Modeling Approach

Case 3 was originally published in the Annex of the German standard *DIN EN 1991-1-1-2/NA*. The reference values given in Table 7 were published in the German standard and verified using Abaqus. A 2D heat transfer model was generated in Abaqus with linear heat transfer elements for a 1m-wide segment of the insulation material. The sides of the 1m by 1m segment of insulation material were insulated to produce a 1D temperature gradient across the thickness of the slab.

The mesh density and time step in the Abaqus model were reduced until the solution converged. The time step Δt was selected for a given element size Δx by setting the Fourier number equal to one, i.e.,

$$\Delta t = \frac{\Delta x^2}{\alpha} \tag{12}$$

where α is the thermal diffusivity. The results from the mesh sensitivity study are shown in Figure 3. It can be seen that the Abaqus solution converges with second-order accuracy (i.e., $O(\Delta x^2)$) due to the simultaneous reduction in spatial and temporal meshes. It was found that the solution converged within 0.1 °C for an element size of 0.01 m and a time step of 0.1 s.

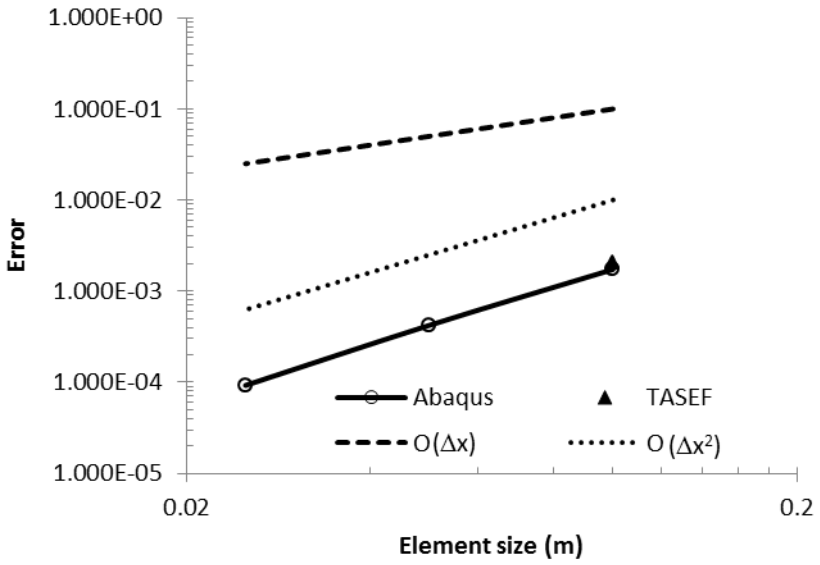

Figure 3. Order of Accuracy for the Abaqus Model

3.3.3 Comparison of Results

The solution published in the Annex of the German standard was compared to the results computed in Abaqus and TASEF. From the results in Table 8, it can be seen that the Abaqus solution matches to solution published in the German standard. The TASEF model also confirms the solution.

Table 8. Comparison between the Abaqus and TASEF models and the published solution

Time (s)	Temperature (°C)			Difference between Abaqus and the Published Solution (°C)
	Published Solution	Abaqus	TASEF	
0	1000	1000.0	1000.0	0.0
60	999.3	999.3	999	0.0
300	891.8	891.8	892	0.0
600	717.7	717.7	718	0.0
900	574.9	574.9	575	0.0
1200	460.4	460.4	461	0.0
1500	368.7	368.7	369	0.0
1800	295.3	295.3	296	0.0

3.4 Case 4 – 1D Axisymmetric Heat Transfer by Convection

3.4.1 Problem Statement

A metal pipe of circular cross section ($k = 50$ W/(m·K), $\rho = 5000$ kg/m^3, $c = 500$ J/(kg·K), $\varepsilon = 0$) is coated with an insulation material ($k = 0.05$ W/(m·K), $\rho = 500$ kg/m^3, $c = 1000$ J/(kg·K), $\varepsilon = 0$). The insulation layer is contained within a 1 mm thick metallic cover with the same properties as the pipe. The inner and outer radii of the pipe are 25 mm and 30 mm, and the inner and outer radii of the insulation layer are 30 mm and 80 mm. The surrounding air temperature is 0 °C, and the temperature of the fluid flowing through the pipe is 1000 °C. The inner and outer heat transfer coefficients are 100 W/(m^2·K) and 10 W/(m^2·K), respectively. Calculate the steady-state temperature at various depths and compare with the values given in Table 9.

Table 9. Reference Values

Radius (mm)	Temperature (°C)
25	981.2
30	981.0
40	710.3
50	500.3
60	328.8
70	183.7
80	58.1
81	58.1

3.4.2 Modeling Approach

The analytical solution was derived for 1D steady state conduction through an axisymmetric pipe with convective boundary conditions at the inner and outer surfaces of the pipe. The thermal resistances R_{hi} and R_{ho} for convection between the fluid and the inner and outer surfaces of the pipe, respectively, are given by:

$$R_{hi} = \frac{1}{2\pi r_i h_i}, \qquad R_{ho} = \frac{1}{2\pi r_o h_o}, \tag{13}$$

where r_i and r_o are the inner and outer radii of the pipe, respectively, and h_i and h_o are the inner and outer heat transfer coefficients, respectively. The thermal resistance $R_{k,j}$ for conduction through a layer j with inner and outer radii $r_{i,j}$ and $r_{o,j}$ is given by:

$$R_{k,j} = \frac{\ln\left(\frac{r_{o,j}}{r_{i,j}}\right)}{2\pi k_j}, \tag{14}$$

where k_j is the conductivity of layer j. The total thermal resistance of the pipe is found by summing the inner and outer convection resistances in Eq. (13) and the conduction resistances in Eq. (14) for each of the layers of the pipe.

The analytical solution was verified by a finite element analysis in Abaqus and TASEF. In particular, a 2D axisymmetric model was generated in Abaqus with linear heat transfer elements for a 1cm section of pipe. A steady state heat transfer analysis was conducted to determine the steady state temperatures in the pipe. A mesh sensitivity study was performed, and it was determined that a mesh density of 0.1cm produced temperatures that were converged to within 0.1 °C. An axisymmetric model was also generated in TASEF using an element size of 0.001 m to verify the analytical and Abaqus solutions.

3.4.3 Comparison of Results

In Table 10, the results from the Abaqus and TASEF analyses are compared to the analytical solution. It can be seen that the temperature difference between the Abaqus model and the analytical solution is less than 0.1 °C. The TASEF solution is within 1 °C of the analytical and Abaqus solutions.

Table 10. Comparison between the analytical solution and the results from Abaqus and TASEF

Radius	Temperature (°C)			Difference between Abaqus and the Analytical Solution (°C)
mm	Analytical Solution	Abaqus	TASEF	
25	981.2	981.2	981	0.0
30	981.0	981.0	981	0.0
40	710.3	710.3	710	0.0
50	500.3	500.4	500	0.1
60	328.8	328.8	329	0.0
70	183.7	183.7	184	0.0
80	58.1	58.1	58	0.0
81	58.1	58.1	58	0.0

3.5 Case 5 – 2D Axisymmetric Heat Transfer by Convection and Radiation

3.5.1 Problem Statement

A metal pipe of circular cross section ($k = 50$ W/(m·K), $\rho = 7850$ kg/m^3, $c = 500$ J/(kg·K), $\varepsilon = 0.8$ penetrates a 0.2 m thick solid wall ($k = 1.5$ W/(m·K), $\rho = 2400$ kg/m^3, $c = 1000$ J/(kg·K), $\varepsilon = 0.8$), as shown in Figure 4. The inner and outer radii of the pipe are 95 mm and 100 mm. The pipe is 2.2 m in length and extends 1 m on each side of the wall. The initial temperature is 20 °C. The inner surface of the pipe is perfectly insulated. The outer surfaces of the pipe and wall are subjected to convection and radiation according to Eq. (4). On one side of the wall, the temperature is 20 °C and the heat transfer coefficient is 4 W/(m^2·K). On the other side of the wall, the temperature is given by the ISO 834 time-temperature curve, Eq. (5), and the heat transfer coefficient is 25 W/(m^2·K). Calculate the temperature at the intersection between the pipe and wall on the unheated surface (as shown in Figure 4) and compare with the values given in Table 11.

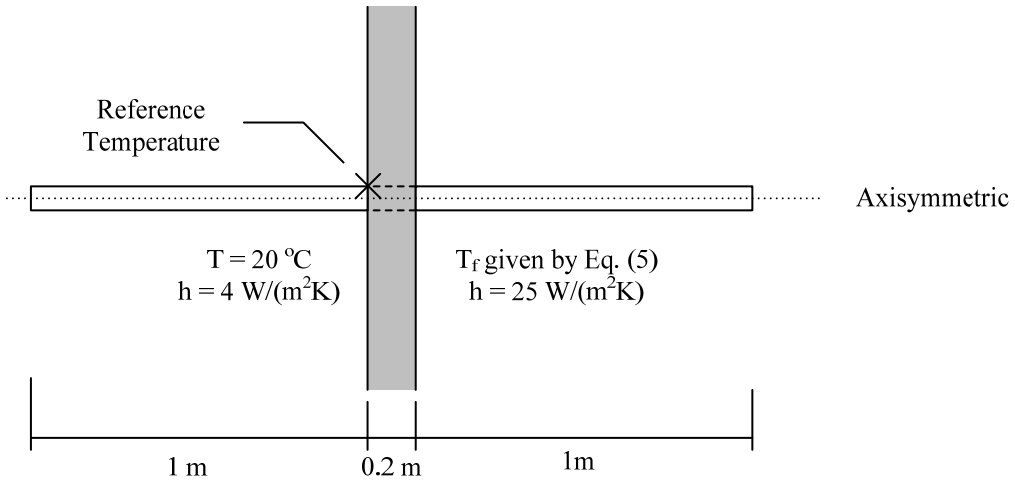

Figure 4

Table 11. Reference Values

Time (h)	Temperature (°C)
0	20
0.5	49
1.0	107
1.5	158
2.0	201

3.5.2 Modeling Approach

Case 5 was modeled in Abaqus using linear axisymmetric heat transfer elements. The solution was verified by finite element analysis in TASEF.

A fine mesh with element sizes of 0.0025 m was used in Abaqus, and the time step was systematically reduced until the solution converged. From the convergence study, the solution was found to converge within 0.3 °C for a time step of 15 s.

3.5.3. Comparison of Results

A comparison between the Abaqus and TASEF solutions is shown in Table 12. It can be seen that the temperature difference between the Abaqus and TASEF models are within 2 °C.

Table 12. Comparison between Abaqus and TASEF

	Temperature (°C)		Temperature Difference between Abaqus and TASEF (°C)
Time (h)	Abaqus	TASEF	
0	20	20	0
0.5	49	47	-2
1.0	107	107	0
1.5	158	159	1
2.0	201	201	0

3.6 Case 6 – 2D Heat Transfer with Cooling by Convection

3.6.1 Problem Statement

A 2 m by 2 m square column ($k = 1$ W/(m·K), $\rho = 1$ kg/m^3, $c = 1$ J/(kg·K), $\varepsilon = 0$) with an initial temperature of 1000 °C cools via convection only. Assuming that $h = 1$ W/(m^2·K) and the surrounding air temperature is 0 °C, calculate the temperature at the center of the column as a function of time and compare to the values given in Table 13.

Table 13. Reference Values

Time (s)	Temperature (°C)
0.0	1000.
0.1	986.4
0.2	903.8
0.4	690.2
0.6	514.7
0.8	382.7
1	284.5

3.6.2 Modeling Approach

The analytical solution for this case was originally published by Wickström and Pålsson (1999). Wickström and Pålsson also provided a numerical solution from the software TASEF. Details about the analysis can be found in the referenced report. A convergence study was performed in TASEF, and it was found that a mesh of 256 elements provided accuracy to within 1 °C.

3.6.3 Comparison of Results

The comparison between TASEF and the analytical solution is reproduced in Table 2. It can be seen that the temperature difference between the analytical and numerical solution is less than 1 °C, which is acceptable given the accuracy the numerical solution from TASEF.

Table 14. Comparison between the Analytical Solution and TASEF

Time (s)	**Temperature (°C)**		**Difference between TASEF and the Analytical Solution (°C)**
	Analytical Solution	**TASEF**	
0.0	1000.	1000	0
0.1	986.4	986	0
0.2	903.8	904	0
0.4	690.2	691	1
0.6	514.7	515	0
0.8	382.7	384	1
1	284.5	285	0

3.7 Case 7 – 2D Heat Transfer by Convection and Radiation

3.7.1 Problem Statement

A 0.2 m by 0.2 m square column ($k = 1$ W/(m·K), $\rho = 2400$ kg/m^3, $c = 1000$ J/(kg·K), $\varepsilon = 0.8$) is heated according to the ISO 834 time-temperature curve, Eq. (5). Assuming that $h = 10$ W/(m^2·K) and that the initial temperature T_∞ is 0 °C, calculate the temperature at the column center, corner and middle side surface as a function of time and compare to the values given in Table 15.

Table 15. Reference Values

Time (min)	Temperature (°C)		
	Center	Side	Corner
0	0	0	0
30	9	721	809
60	127	873	921
90	315	952	984
120	492	1005	1028
150	640	1045	1062
180	757	1077	1089

3.7.2 Modeling Approach

Case 7 was originally published by Wickström and Pålsson (1999). The solution published by Wickström and Pålsson was based on a TASEF model that had converged with 2 °C accuracy. The solution was verified by Abaqus using a 2D finite element model with linear heat transfer elements. The mesh density and time step in the Abaqus model were reduced until the solution converged. The time step Δt was selected for a given element size Δx by Eq. (12). Figure 5 illustrates that the model exhibits second-order accuracy (i.e., $O(\Delta x^2)$). From the convergence study, the Abaqus model was found to converge within 1°C for a mesh density of 0.001 m and time step of 2.4 s.

3.7.3 Comparison of Results

The results from TASEF and Abaqus are compared in Table 16. It can be seen that the calculated temperatures are within 2 °C.

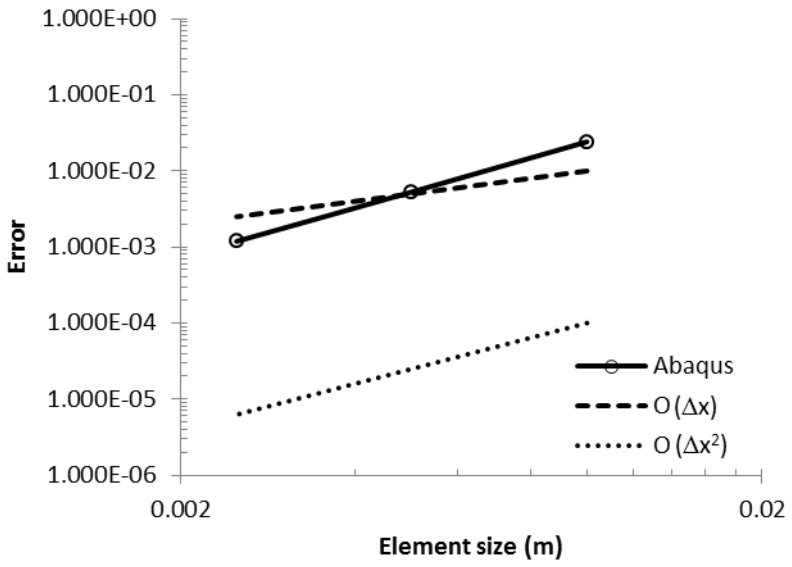

Figure 5. Order of Accuracy of Abaqus Model

Table 16. Comparison between TASEF and Abaqus

Time (min)	Temperature (°C)						Temperature Difference between TASEF and Abaqus (°C)		
	Abaqus			TASEF					
	Center	Side	Corner	Center	Side	Corner	Center	Side	Corner
0	0	0	0	0	0	0	0	0	0
30	9	721	809	10	723	811	1	2	2
60	127	873	921	128	873	922	1	0	1
90	315	952	984	315	952	984	0	0	0
120	492	1005	1028	492	1006	1028	0	1	0
150	640	1045	1062	639	1046	1062	-1	1	0
180	757	1077	1089	756	1077	1089	-1	0	0

3.8 Case 8 – 2D Heat Transfer with Temperature-Dependent Conductivity

3.8.1 Problem Statement

A 0.2 m by 0.2 m square column ($\rho = 2400$ kg/m^3, $c = 1000$ J/(kg·K), $\varepsilon = 0.8$) is heated according to the ISO 834 time-temperature curve, Eq. (5). The thermal conductivity of the column material varies linearly with temperature such that its value is 1.5 W/(m·K) at 0 °C, 0.7 W/(m·K) at 200 °C, and 0.5 W/(m·K) at 1000 °C. Assuming that $h = 10$ W/(m^2·K) and that the initial air temperature is 0 °C, calculate the temperature at the column center, corner and middle side surface as a function of time and compare to the values given in Table 17.

Table 17. Reference Values

Time (min)	Temperature (°C)		
	Center	Side	Corner
0	0	0	0
30	18	743	815
60	99	884	923
90	190	958	985
120	300	1008	1028
150	411	1046	1062
180	512	1077	1089

3.8.2 Modeling Approach

Case 8 was originally published by Wickström and Pålsson (1999). The solution published by Wickström and Pålsson was based on a TASEF model that had converged with 1 °C accuracy. The solution was verified by Abaqus using a 2D finite element model with linear heat transfer elements. The mesh density and time step in the Abaqus model were reduced until the solution converged. The time step Δt was selected for a given element size Δx by Eq. (12). From the convergence study, the Abaqus model was found to converge within 1°C for a mesh density of 0.001 m and time step of 2.4 s.

3.8.3 Comparison of Results

The results from TASEF and Abaqus are compared in Table 18. It can be seen that the calculated temperatures are within 2 °C.

Table 18. Comparison between TASEF and Abaqus

Time (min)	Temperature (°C)						Temperature Difference between TASEF and Abaqus (°C)		
	Abaqus			TASEF					
	Center	Side	Corner	Center	Side	Corner	Center	Side	Corner
0	0	0	0	0	0	0	0	0	0
30	18	743	815	18	744	815	0	1	0
60	99	884	923	99	884	923	0	0	0
90	190	958	985	189	958	985	-1	0	0
120	300	1008	1028	299	1009	1028	-1	1	0
150	411	1046	1062	409	1047	1062	-2	1	0
180	512	1077	1089	510	1077	1089	-2	0	0

3.9 Case 9 – 2D Heat Transfer in a Composite Section with Temperature-Dependent Conductivity

3.9.1 Problem Statement

A hollow square metal tube ($\rho = 7850$ kg/m^3, $c = 600$ J/(kg·K), $\varepsilon = 0.8$) is filled with an insulation material ($k = 0.05$ W/(m·K), $\rho = 50$ kg/m^3, $c = 1000$ J/(kg·K), $\varepsilon = 0$). The thermal conductivity of the metal tube varies linearly with temperature such that its value is 54.7 W/(m·K) at 0 °C, 27.3 W/(m·K) at 800 °C, and 27.3 W/(m·K) at 1200 °C. The tube walls are 0.5 mm thick, and the exterior width of the assembly is 0.201 m. The surrounding air temperature is 1000 °C, and the initial temperature of the assembly is 0 °C. Assuming that the heating is by convection and radiation, Eq. (4), and that the heat transfer coefficient is 10 W/(m^2·K), calculate the temperature at the center of the tube as a function of time and compare with the values given in Table 19.

Table 19. Reference Values

Time (min)	Temperature (°C)
0	0
30	341
60	723
90	886
120	953
150	981
180	992

3.9.2 Modeling Approach

Case 9 was published in the verification report by Wickström and Pålsson (1999) and also appeared in the Annex of the German standard *DIN EN 1991-1-1-2/NA*. Because of slight differences between the two published solutions, the problem was modeled in Abaqus. The reference values that appear in Table 19 are taken from Wickström and Pålsson (1999), which were based on a 2D finite element analysis in TASEF that had converged with 2 °C accuracy.

A 2D finite element model was generated in Abaqus using linear heat transfer elements. Due to the small thickness (i.e., 0.5 mm) of the metal tube in relation to the overall dimension of the assembly, a fine mesh of 0.00025 m was specified for the metal tube while the mesh over the insulation was varied from coarse (i.e., Δx = 0.01 m) to fine (i.e., Δx = 0.001 m). Compatibility between the finely meshed metal tube and coarsely meshed insulation was achieved by imposing a tie constraint at the interface between the metal tube and insulation. The time step Δt was calculated by Eq. (12) based on the element size Δx and thermal diffusivity α for the insulation material. The solution converged within 1°C for a mesh density of 0.001 m and time step of 1 s.

3.9.3 Comparison of Results

The results from the German standard are compared to the TASEF and Abaqus models in Table 20. It can be seen that the Abaqus and TASEF models compare well, with the temperature difference being within 2 °C. The difference is larger between the German standard and the TASEF and Abaqus models, particularly at 60 and 90 min.

Table 20. Comparison between TASEF and Abaqus

Time (min)	Temperature (°C)			Difference between Abaqus and TASEF (°C)
	DIN EN 1991-1-1-2	TASEF	Abaqus	
0	0	0	0	0
30	341	343	341	-2
60	717	722	723	1
90	882	885	886	1
120	951	952	953	1
150	979	980	981	1
180	992	992	992	0

3.10 Case 10 – 2D Axisymmetric Heat Transfer with Non-Uniform Heat Flux

3.10.1 Problem Statement

A bar with circular cross section of diameter 20 cm and length 200 cm ($k = 50\ \mathrm{W/(m{\cdot}K)}$, $\rho = 7850\ \mathrm{kg/m^3}$, $c = 500\ \mathrm{J/(kg{\cdot}K)}$, $\varepsilon = 0.8$) is heated uniformly over half of its length by an incident radiant heat flux of 30 kW/m^2 with convection to ambient, Eq. (6). The remaining half of the bar's length is cooled by convection and radiation to ambient. The surrounding air temperature over the entire length of the bar is 20 °C, and the initial temperature of the bar is 20 °C. Assuming that the heat transfer coefficient is 10 W/(m^2·K) and that the ends of the bar are perfectly insulated, calculate the temperature along the center of the bar at 60 min for the locations given in Table 21.

Table 21. Reference Values

Distance (cm)	Temperature (°C)
0	357
25	357
50	353
75	325
100	195
125	59
150	25
175	20
200	20

3.10.2 Modeling Approach

Case 10 was modeled in Abaqus using linear axisymmetric heat transfer elements. The solution was verified by finite element analysis in TASEF.

The mesh density and time step in the Abaqus model were reduced until the solution converged. The time step Δt was selected for a given element size Δx by Eq. (12). The results of the convergence study are shown in Figure 6. The solution was found to converge within 0.2 °C for a mesh density of 0.005 m.

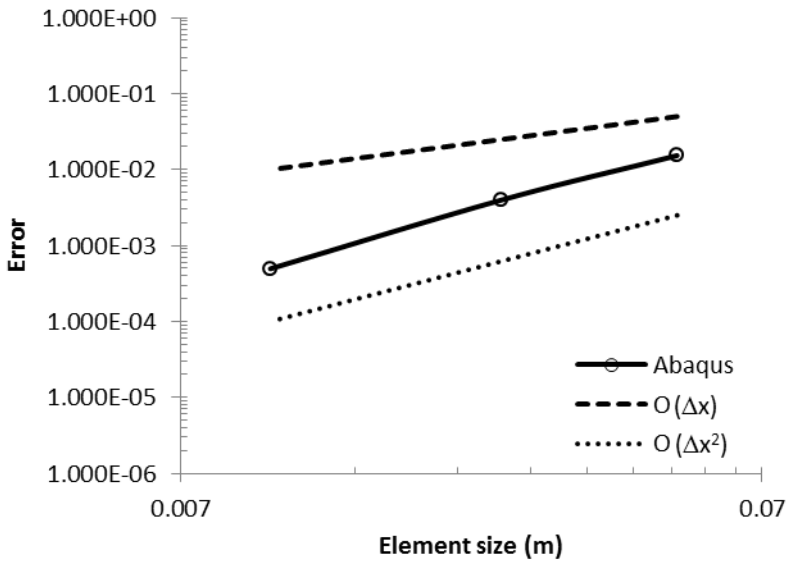

Figure 6. Convergence of the Abaqus model

3.10.3 Comparison of Results

The TASEF model was run with increasingly fine mesh until the solution converged. The TASEF results are compared to the Abaqus results in Table 22. It can be seen that the temperature difference is within 1 °C.

Table 22. Comparison between TASEF and Abaqus

x (cm)	Temperature (°C)		Difference between Abaqus and TASEF (°C)
	Abaqus	TASEF	
0	357	357	0
25	357	357	0
50	353	353	0
75	325	325	0
100	195	195	0
125	59	58	-1
150	25	25	0
175	20	21	1
200	20	20	0

3.11 Case 11 – Lumped Mass with Moisture Evaporation

3.11.1 Problem Statement

A 1 cm by 1 cm square column (dry properties: $\rho = 2400$ kg/m^3, $c = 1000$ J/(kg·K), $\varepsilon = 0.8$) is heated according to the ISO 834 time-temperature curve, Eq. (5). If the thermal conductivity of the material is relatively large, the temperature in the section, T, can be taken as uniform. The column contains 2.08 % water by mass that evaporates at temperatures between 100 °C and 120 °C. The density of water and specific heat capacity of water can be taken as 1000 kg/m^3 and 4187 J/(kg·K), respectively. The latent heat of evaporation (2260 kJ/(kg of water)) is assumed to be in addition to the specific heat of the material. During evaporation, the amount of water is assumed to decrease linearly to zero. Assuming that $h = 10$ W/(m^2·K) and that the initial temperature is 20 °C, calculate the temperature of the column as a function of time and compare to the values given in Table 23.

Table 23. Reference Values

Time (min)	Temperature (°C)
0	20
1	83
2	112
3	148
4	192
5	225
6	249
7	266
8	278
9	285
10	291
15	299

3.11.2 Modeling Approach

The problem was modeled in Abaqus using 2D linear heat transfer elements and verified by TASEF. Because Abaqus does not have a lumped mass model, a 2D finite element model was generated with linear heat transfer elements and uniform temperature was imposed throughout the model using a tie constraint.

Temperature-dependent material properties were specified according to the problem statement. The effect of moisture on the density and specific heat was modeled in Abaqus using an effective specific heat c_{eff} that was calculated from the enthalpy. In particular, the effective specific heat was calculated according to

$$c_{eff} = \frac{\rho_c c_c + \rho_w c_w}{\rho_{eff}} \tag{15}$$

where ρ_c and c_c are the density and specific heat of the dry cementitious material; ρ_w and c_w are the density and specific heat of moisture, which vary in time due to evaporation; and ρ_{eff} is an effective density, which was taken as the dry density of the cementitious material. The latent heat of evaporation was specified as a material property with solidus and liquidus temperatures respectively given as the lower and upper temperatures for the moisture evaporation. Abaqus adds the latent heat effect to the specific heat capacity by default. TASEF allows the enthalpy to be specified directly as a temperature-dependent material property. Therefore, there is no need to define effective density and heat capacity to account for the presence of moisture. Although the material properties are defined differently in Abaqus and TASEF, the programs are expected to yield the same result because they are solving the same heat transfer equation for two materials that have equivalent thermal properties.

A convergence study was performed, as shown in Figure 7. A time step of 1 s resulted in a solution that converged with 0.3 °C accuracy in the Abaqus model.

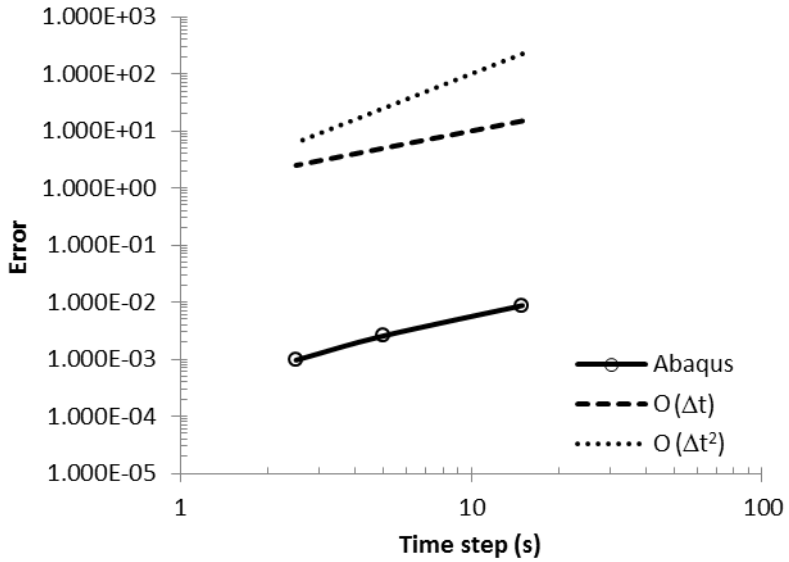

Figure 7. Convergence study in Abaqus

3.11.3 Comparison of Results

The results from Abaqus and TASEF are compared in Table 28. It can be seen that the results are in good agreement, with temperature differences no greater than 1 °C.

Table 24. Comparison between TASEF and Abaqus

Time min	Temperature °C		Temperature Difference between TASEF and Abaqus °C
	Abaqus	TASEF	
0	20	20	0
1	83	83	0
2	112	112	0
3	148	148	0
4	192	192	0
5	225	225	0
6	249	250	-1
7	266	266	0
8	278	278	0
9	285	286	-1
10	291	291	0
15	299	299	0

3.12 Case 12 – 1D Heat Transfer with Moisture Evaporation

3.12.1 Problem Statement

A 16 cm thick wall (dry properties: $\rho = 500$ kg/m^3, $c = 800$ J/(kg·K), $k = 0.1$ W/(m·K), $\varepsilon = 0.8$) is heated on both sides according to the ISO 834 time-temperature curve, Eq. (5). The water content of the wall is 10 % by mass, and the water is assumed to evaporate between 100 °C and 110 °C. The density of water and specific heat capacity of water can be taken as 1000 kg/m^3 and 4187 J/(kg·K), respectively. The latent heat of evaporation (2260 kJ/(kg of water)) is assumed to be in addition to the specific heat of the material. During evaporation, the amount of water is assumed to decrease linearly to zero. Assuming that $h = 25$ W/(m^2·K) and that the initial temperature is 20 °C, calculate the temperature at various depths as a function of time and compare to the values given in Table 25.

Table 25. Reference Values

Time (min)	Temperature (°C)		
	Surface	4 cm	Center
0	20	20	20
15	717	24	20
30	829	50	20
45	893	83	24
60	938	133	33
75	972	206	46
90	1001	268	62
105	1024	323	80
120	1045	371	94

3.12.2 Modeling Approach

A 1 cm segment of the wall was modeled in Abaqus using 2D linear heat transfer elements and verified by TASEF.

Temperature-dependent material properties were specified according to the problem statement. The effect of moisture on the density and specific heat was modeled in Abaqus using an effective specific heat c_{eff} that was calculated from the enthalpy according to Eq. (15). The latent heat of evaporation was specified as a material property with solidus and liquidus temperatures respectively given as the lower and upper temperatures for the moisture evaporation. Abaqus adds the latent heat effect to the specific heat capacity by default. TASEF allows the enthalpy to be specified directly as a temperature-dependent material property. Therefore, there is no need to define effective density and heat capacity to account for the presence of moisture.

The mesh density and time step in the Abaqus model were reduced according to Eq. (12). It was found that the model converged within 0.3 °C for an element size of 0.0005 m and a time step of 0.25 s.

3.12.3 Comparison of Results

Results between TASEF and Abaqus are compared in Table 26. It can be seen that the Abaqus and TASEF solutions are within 1 °C.

Table 26. Comparison between TASEF and Abaqus

Time (min)	Temperature (°C)						Difference between Abaqus and TASEF (°C)		
	TASEF			Abaqus					
	Surface	4 cm	Center	Surface	4 cm	Center	Surface	4 cm	Center
0	20	20	20	20	20	20	0	0	0
15	717	24	20	717	24	20	0	0	0
30	829	50	20	829	50	20	0	0	0
45	893	83	24	893	83	24	0	0	0
60	938	133	33	938	133	33	0	0	0
75	972	206	46	972	206	46	0	0	0
90	1001	268	63	1001	268	62	0	0	-1
105	1024	323	80	1024	323	80	0	0	0
120	1045	371	94	1045	371	94	0	0	0

3.13 Case 13 – 2D Heat Transfer with Moisture Evaporation

3.13.1 Problem Statement

A 0.2 m by 0.2 m square column (dry properties: $\rho = 2400$ kg/m^3, $c = 1000$ J/(kg·K), $\varepsilon = 0.8$) is heated according to the ISO 834 time-temperature curve, Eq. (5). The thermal conductivity of the column material varies linearly with temperature such that its value is 1.5 W/(m·K) at 0 °C, 0.7 W/(m·K) at 200 °C, and 0.5 W/(m·K) at 1000 °C. The column contains 2.08 % water by mass that evaporates at temperatures between 100 °C and 120 °C. The density of water and specific heat capacity of water can be taken as 1000 kg/m^3 and 4187 J/(kg·K), respectively. The latent heat of evaporation (2260 kJ/(kg of water)) is assumed to be in addition to the specific heat of the material. During evaporation, the amount of water is assumed to decrease linearly to zero. Assuming that $h = 10$ W/(m^2·K) and that the initial temperature is 20 °C, calculate the temperature at the column center, corner and middle side surface as a function of time and compare to the values given in Table 27.

Table 27. Reference Values

Time (min)	Temperature (°C)		
	Center	Side	Corner
0	20	20	20
30	31	764	835
60	85	904	943
90	147	978	1005
120	272	1028	1048
150	393	1066	1082
180	500	1097	1109

3.13.2 Modeling Approach

The problem was modeled in Abaqus using 2D linear heat transfer elements and verified by TASEF. Due to symmetry, a quarter of the section was modeled.

Temperature-dependent material properties were specified according to the problem statement. The effect of moisture on the density and specific heat was modeled in Abaqus using an effective specific heat c_{eff} that was calculated from the enthalpy according to Eq. (15). The latent heat of evaporation was specified as a material property with solidus and liquidus temperatures respectively given as the lower and upper temperatures for the moisture evaporation. Abaqus adds the latent heat effect to the specific heat capacity by default. TASEF allows the enthalpy to be specified directly as a temperature-dependent material property. Therefore, there is no need to define effective density and heat capacity to account for the presence of moisture.

The mesh density and time step in the Abaqus model were reduced according to Eq. (12). It was found that the model converged to within 1.1 °C for an element size of 0.001 m and a time step of 2.4 s.

3.13.3 Comparison of Results

The results from Abaqus and TASEF are compared in Table 28. It can be seen that the results are in good agreement, with temperature differences no greater than 1 °C.

Table 28. Comparison between TASEF and Abaqus

Time (min)	Temperature (°C)						Difference between TASEF and Abaqus (°C)		
	TASEF			Abaqus					
	Center	Side	Corner	Center	Side	Corner	Center	Side	Corner
0	20	20	20	20	20	20	0	0	0
30	30	765	836	31	764	835	1	-1	-1
60	85	904	943	85	904	943	0	0	0
90	146	978	1005	147	978	1005	1	0	0
120	272	1028	1048	272	1028	1048	0	0	0
150	393	1066	1082	393	1066	1082	0	0	0
180	500	1097	1109	500	1097	1109	0	0	0

3.14 Case 14 – 2D Heat Transfer in a Composite Section with Moisture Evaporation and Temperature-Dependent Conductivity

3.14.1 Problem Statement

A hollow metal square tube ($\rho = 7850$ kg/m^3, $c = 600$ J/(kg·K), $\varepsilon = 0.8$) is filled with a cementitious material. The tube walls are 10 mm thick, and the exterior dimensions are 220 mm x 220 mm. The thermal conductivity of the tube is 54.7 W/(m·K) at 0 °C and decreases linearly to 27.3 W/(m·K) at 800 °C and remains at this same value for higher temperatures. The cementitious material ($\rho = 2400$ kg/m^3, $c = 1000$ J/(kg·K)) contains 2.08 % water by mass that evaporates between 100 °C and 120 °C. The density of water and specific heat capacity of water can be taken as 1000 kg/m^3 and 4187 J/(kg·K), respectively. The latent heat of evaporation (2260 kJ/(kg of water)) is assumed to be in addition to the specific heat of the material. During evaporation, the amount of water is assumed to decrease linearly to zero. The thermal conductivity of the cementitious material varies linearly with temperature such that its value is 1.5 W/(m·K) at 0 °C, 0.7 W/(m·K) at 200 °C, and 0.5 W/(m·K) at 1000 °C. The surrounding air temperature is 1000 °C, and the initial temperature of the column is 0 °C. Assuming that the heat transfer coefficient is 10 W/(m^2·K), calculate the temperature at the center, side and corner of the concrete portion of the column as a function of time and compare with the values given in Table 29.

Table 29. Reference Values

Time (min)	Temperature (°C)		
	Center	Side	Corner
0	0	0	0
30	19	951	981
60	90	971	990
90	177	979	994
120	309	984	995
150	426	988	996
180	524	990	997

3.14.2 Modeling Approach

The problem was modeled in Abaqus using 2D linear heat transfer elements and verified by TASEF. Due to symmetry, a quarter of the section was modeled.

Temperature-dependent material properties were specified according to the problem statement. The effect of moisture on the density and specific heat was modeled in Abaqus using an effective specific heat c_{eff} that was calculated from the enthalpy according to Eq. (15). The latent heat of evaporation was specified as a material property with solidus and liquidus temperatures respectively given as the lower and upper temperatures for the moisture evaporation. Abaqus adds the latent heat effect to the specific heat capacity by default. TASEF allows the enthalpy to

be specified directly as a temperature-dependent material property. Therefore, there is no need to define effective density and heat capacity to account for the presence of moisture.

A fine mesh was specified for the metal tube, while the mesh density and time step for the cementitious material were reduced according to Eq. (12) in the Abaqus model. It was found that the model converged to within 0.6 °C for an element size of 0.001 m and a time step of 2.4 s.

3.14.3 Comparison of Results

The results from Abaqus and TASEF are compared in Table 30. It can be seen that the results are in reasonable agreement, with errors no greater than 3 °C.

Table 30. Comparison between TASEF and Abaqus

Time (min)	Temperature (°C)						Difference between Abaqus and TASEF (°C)		
	TASEF			Abaqus					
	Center	Side	Corner	Center	Side	Corner	Center	Side	Corner
0	0	0	0	0	0	0	0	0	0
30	20	952	981	19	951	981	-1	-1	0
60	91	971	991	90	971	990	-1	0	-1
90	175	979	994	177	979	994	2	0	0
120	306	984	995	309	984	995	3	0	0
150	423	988	996	426	988	996	3	0	0
180	521	990	997	524	990	997	3	0	0

3.15 Case 15 – 2D Heat Transfer in a Composite Section with Cavity Radiation

3.15.1 Problem Statement

A metal I-beam ($\rho = 7850$ kg/m^3, $c = 600$ J/(kg·K), $\varepsilon = 0.8$) is protected by a 1 cm thick insulation board ($\rho = 870$ kg/m^3, $c = 1130$ J/(kg·K), $\varepsilon = 0.8$) as shown in Figure 8. The I-beam fits within a square area 200 mm by 200 mm, its flanges are 15 mm thick, and its web is 9 mm thick. There is a 10 mm air gap between the boards and the adjacent flanges. The thermal conductivity of the insulation board is 0.174 W/(m·K) at 0 °C and increases linearly to 0.188 W/(m·K) at 250 °C and remains at this same value for higher temperatures. The thermal conductivity of the metal varies linearly with temperature such that its value is 54.0 W/(m·K) at 20 °C, 27.3 W/(m·K) at 800 °C, and 27.3 W/(m·K) at 1200 °C. The fire is represented by the ISO 834 time-temperature curve, Eq. (5), with an initial temperature of 20 °C. The convection heat transfer coefficient to the exterior of the insulation board is 10 W/(m^2·K), but it is assumed that there is no convective heat transfer at the interior surfaces of the boards or the I-beam. Calculate the temperature at the center of either flange as a function of time and compare to the values given in Table 31.

Table 31. Reference Values

Time (min)	Temperature (°C)
0	20
30	229
60	519
90	736
120	879

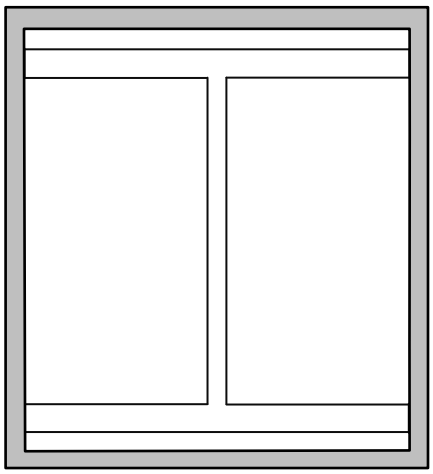

Figure 8

3.15.2 Modeling Approach

Case 15 was originally published in the verification report by Wickström and Pålsson (1999). Wickström and Pålsson also presented the solution calculated by a 2D finite element analysis in TASEF that had converged with 2 °C accuracy. The problem was also modeled using the software HEATING 7.3 (Trelles et al., 2003). Because of slight differences between the two published solutions, the problem was modeled in Abaqus as well.

In the Abaqus model, 2D linear heat transfer elements were used to model one quarter of the cross-section based on symmetry in the problem. Cavity radiation with reflection symmetry was employed in Abaqus using the default parameters for view factor calculations. Equation (12) was not used to simultaneously refine the mesh and time step due to the temperature-dependent thermal conductivity and the nonlinear radiation boundary conditions in the cavities. Instead, a fine mesh (i.e., four elements over the thickness of the insulation, flange, and web, respectively) was specified for the entire model and the time step was systematically reduced until the solution converged. The solution converged with 1 °C accuracy at a time step of 15 s. To ensure that the mesh was adequate for convergence, the analysis was repeated with a time step of 15 s and a finer mesh of eight elements over the thickness of the insulation, flange, and web, respectively. It was found that the temperature difference was less than 1 °C, demonstrating that the mesh of four elements over the thickness of the insulation, flange, and web was sufficient.

3.15.3 Comparison of Results

The temperature at the center of the flange is given in Table 32 for the analyses in TASEF, HEATING 7.3, and Abaqus. It can be seen that the three methods agree well, with temperature differences of no more than 4 °C (i.e., less than 2% error).

Table 32. Comparison between TASEF, HEATING 7.3, and Abaqus

Time (min)	Temperature (°C)			Difference between Abaqus and TASEF (°C)	Difference between Abaqus and HEATING (°C)
	TASEF	HEATING 7.3	Abaqus		
0	20	20	20	0	0
30	226	230	229	3	-1
60	518	521	519	1	-2
90	736	738	736	0	-2
120	879	880	879	0	-1

3.16 Case 16 – 3D Heat Transfer with Non-Uniform Heat Flux

3.16.1 Problem Statement

Consider a 1.0 m by 2.0 m rectangular metal plate ($k = 50$ W/(m·K), $\rho = 7850$ kg/m^3, $c = 500$ J/(kg·K), $\varepsilon = 0.8$) that is 0.10 m thick. In Cartesian coordinates (x, y), the corners of the plate are (0,0), (1,0), (1,2), and (0,2). A lower quarter of the plate front surface whose corners are (0,0), (0.5,0), (0.5,1), (0,1) is heated with an incident radiant heat flux of 30 kW/m^2 with reradiation to the surroundings and convection with surrounding air, Eq. (6). The remainder of the front surface and the entire back surface have only reradiation to the surroundings and convection with the surrounding air. The sides of the plate are insulated. The surroundings and air temperature are both at 20^{o}C, while the heat transfer coefficient at the plate surface is 10 W/(m^2·K). Calculate the temperature at the mid-depth along the height of the plate at $x = 0.25$ m and along the width of the plate at $y = 0.5$ m after a 60 minute exposure. Compare the results with the values given in Table 33.

Table 33. Reference Values

x (m)	*y* (m)	*z* (m)	Temperature (°C)
0.25	0.00	0.05	183
0.25	0.25	0.05	182
0.25	0.50	0.05	181
0.25	0.75	0.05	167
0.25	1.00	0.05	102
0.25	1.25	0.05	37
0.25	1.50	0.05	22
0.25	1.75	0.05	20
0.25	2.00	0.05	20
0.00	0.50	0.05	194
0.25	0.50	0.05	181
0.50	0.50	0.05	111
0.75	0.50	0.05	39
1.00	0.50	0.05	25

3.16.2 Modeling Approach

The problem was modeled in Abaqus using 3D linear heat transfer elements and verified by ANSYS (2011) and Autodesk Simulation Multiphysics (2012).

The mesh density and time step in the Abaqus model were reduced until the solution converged. The time step Δt was selected for a given element size Δx by Eq. (12). The solution converged within 0.5 °C for a mesh density of 0.0125 m and time step of 12.5 s.

3.16.3 Comparison of Results

The temperature is given in Table 32 for the analyses in Autodesk Simulation Multiphysics (ASM), ANSYS, and Abaqus. It can be seen that the three methods agree well, with temperature differences of no more than 0.5 °C.

Table 34. Comparison between Autodesk Simulation Multiphysics, ANSYS, and Abaqus

x (m)	*y* (m)	*z* (m)	Temperature (°C)			Difference between Abaqus and ASM (°C)	Difference between Abaqus and ANSYS (°C)
			ASM	ANSYS	Abaqus		
0.25	0.0	0.05	182.4	182.2	182.6	0.2	0.4
0.25	0.25	0.05	182.3	182.0	182.5	0.2	0.5
0.25	0.50	0.05	180.4	180.1	180.6	0.2	0.5
0.25	0.75	0.05	166.8	166.5	166.9	0.1	0.4
0.25	1.0	0.05	102.3	102.2	102.3	0.0	0.2
0.25	1.25	0.05	36.7	36.7	36.7	0.0	0.0
0.25	1.50	0.05	22.2	22.3	22.2	0.0	-0.1
0.25	1.75	0.05	20.2	20.2	20.2	0.0	0.0
0.25	2.0	0.05	20.0	20.0	20.0	0.0	0.0
0.0	0.50	0.05	193.7	193.4	193.9	0.2	0.5
0.25	0.50	0.05	180.4	180.1	180.6	0.2	0.5
0.5	0.50	0.05	110.6	110.4	110.6	0.0	0.2
0.75	0.50	0.05	39.4	39.4	39.4	0.0	0.0
1.0	0.50	0.05	25.3	25.4	25.2	-0.1	-0.3

References

Abaqus, v. 6-11, Dassault Systemes Simulia Corporation, Providence, RI, 2011.

ANSYS, *ANSYS Mechanical APDL Theory Reference, Release 14.0,* ANSYS Inc. Canonsburg, PA, USA, 2011.

Autodesk Simulation Multiphysics 2013, Autodesk, Inc., 2012.

Carslaw, H.S. and Jaeger, J.C., Conduction of Heat in Solids, 2nd edition, Oxford University Press, 1969.

Jeffers, A.E. "Heat Transfer Element for Modeling the Thermal Response of Non-Uniformly Heated Plates," *Finite Elements in Analysis and Design*, 63, 62-68, 2013.

Jeffers, A.E., and Sotelino, E.D. "Fiber Heat Transfer Element for Modeling the Thermal Response of Structures in Fire," *Journal of Structural Engineering*, 135, 1191-1200, 2009.

Lattimer, B.Y., "Heat Fluxes from Fires to Surfaces," *The SFPE Handbook of Fire Protection Engineering*, 4th edition, National Fire Protection Association, Quincy, Massachusetts, 2008.

National Annex – Nationally determined parameters – Eurocode 1: Actions on structures – Part 1-2: General actions – Actions on structures exposed to fire, *DIN EN 1991-1-1-2/NA*, Deutsches Institut für Normung (DIN), Berlin, 2010.

Sterner, E., and Wickström, U., *TASEF – Temperature Analysis of Structures Exposed to Fire*, SP Report 1990:05, Swedish National Testing and Research Institute, Borås, 1990.

Trelles, J., Hunt, S.P., and Williams, F.W., *Verifying HEATING 7.3 Against the Swedish National Testing and Research Institute's Suite of Fire Resistance Examples*, Hughes Associates, Inc., Baltimore, MD, 2003.

Wickström, U., "Methods for Predicting Temperatures in Fire-Exposed Structures," *The SFPE Handbook of Fire Protection Engineering*, 4th edition, National Fire Protection Association, Quincy, Massachusetts, 2008.

Wickström, U., and Pålsson, J., *A Scheme for Verification of Computer Codes for Calculating Temperature in Fire Exposed Structures*, SP Report 1999:36, SP Swedish National Testing and Research Institute, Borås, Sweden, 1999.